BNL-213779-2020-JAAM

High-throughput operando-ready X-ray absorption spectroscopy flow reactor cell for powder samples

J. D. Kammert, R. Acevedo-Esteves

To be published in "Review of Scientific Instruments"

January 2020

Photon Sciences

Brookhaven National Laboratory

U.S. Department of Energy

USDOE Office of Science (SC), Basic Energy Sciences (BES) (SC-22)

Notice: This manuscript has been authored by employees of Brookhaven Science Associates, LLC under Contract No. DE-SC0012704 with the U.S. Department of Energy. The publisher by accepting the manuscript for publication acknowledges that the United States Government retains a non-exclusive, paid-up, irrevocable, world-wide license to publish or reproduce the published form of this manuscript, or allow others to do so, for United States Government purposes.

DISCLAIMER

This report was prepared as an account of work sponsored by an agency of the United States Government. Neither the United States Government nor any agency thereof, nor any of their employees, nor any of their contractors, subcontractors, or their employees, makes any warranty, express or implied, or assumes any legal liability or responsibility for the accuracy, completeness, or any third party's use or the results of such use of any information, apparatus, product, or process disclosed, or represents that its use would not infringe privately owned rights. Reference herein to any specific commercial product, process, or service by trade name, trademark, manufacturer, or otherwise, does not necessarily constitute or imply its endorsement, recommendation, or favoring by the United States Government or any agency thereof or its contractors or subcontractors. The views and opinions of authors expressed herein do not necessarily state or reflect those of the United States Government or any agency thereof.

High-Throughput *Operando*-Ready X-Ray Absorption Spectroscopy Flow Reactor Cell for Powder Samples

James D. Kammert[a], Gordon Brezicki[a], Raul Acevedo-Esteves[b], Eli Stavitski[b], Robert J. Davis[a]

a. University of Virginia Department of Chemical Engineering, 102 Engineer's Way, PO Box 400741, Charlottesville, VA 22904-4741, United States

b. National Synchrotron Light Source II, Brookhaven National Lab, Upton, NY 11973, United States

* To whom correspondence should be addressed.

Email: rjd4f@virginia.edu

Abstract

A high-throughput, *operando*-ready X-ray absorption spectroscopy catalytic reaction cell consisting of 4 parallel reactors was designed to collect X-ray absorption near edge structure (XANES) and extended fine structure (EXAFS) spectra under reaction conditions. The cell is capable of operating at temperatures from ambient conditions up to 773 K and pressures from ambient to 2 MPa in a variety of gas environments. The cell design is mechanically simple, and programmable operation at beamline 8-ID (NSLS-II, Brookhaven National Lab) makes it straightforward to use. Reactor tube parts were available as-fabricated from commercial sources, while the heating jacket and cell mounting required custom machining.

1. Introduction

X-ray absorption spectroscopy (XAS) is a well-established technique for obtaining structural and electronic information about transition metal compounds. It is among a small but growing number of techniques that offers the opportunity to gain insights into the atomic structure and chemical state of reacting systems under true reaction conditions. The investigation of heterogeneous catalysts under operating conditions, utilizing *in situ* or *operando* techniques, is highly desirable to interrogate the active chemical state of catalysts,[1] how catalysts evolve with time on stream,[2] and even the structure of single-site catalysts in zeolites.[3] Indeed, the use of *in situ* XAS in the field of heterogeneous catalysis has become a standard practice. Additional examples and more information can be found in the recent review by Bordiga et al. detailing the use of *in situ* X-ray techniques.[4]

The latest generation of synchrotron facilities has state-of-the art technology that utilizes high fluxes of monochromatic X-rays beams. The scan time required to obtain a single absorption spectrum has been reduced from hours to minutes and even subseconds using standard ion chamber

X-ray detectors and fast scanning monochromators. By utilizing faster data collection, it may be possible to use larger datasets to produce greater insights into the chemical and electronic structure of catalytic materials.[5] As a consequence of decreased scan times, however, counting photons is no longer the rate-limiting step in data collection. The introduction of appropriately prepared samples into the X-ray beam is now more time-consuming than the collection of spectra.

Heterogeneous catalysts often consist of loose powders or pellets that must be reshaped into appropriately thin, fragile wafers. These samples are time-consuming to produce and are not optimal for *in situ* or *operando* investigation as they may crack due to temperature, pressure, or flow rate changes. Moreover, dense pellets result in mass transfer effects on the measured rates of product formation. To investigate the behavior of heterogenous catalyst systems under reaction conditions, a number of design constraints must be considered. Reactions often occur at high temperatures, in pressures ranging from near vacuum to tens of MPa, and frequently take place in chemically-harsh environments. To draw meaningful conclusions about catalyst performance, accurate control of the temperature, pressure, and gas flow rate through each catalyst bed must be achieved. Robust construction materials that can withstand a wide range of temperatures and pressures are required, and the reactor must be made of materials that will not react and degrade under experimental conditions. If *operando* measurements are desired, the cell should allow for optimization of the loading of catalyst for spectroscopic analysis and the amount of product formed. Furthermore, the cell must meet stringent safety requirements demanded by the latest generation of synchrotron user facilities, where user safety is paramount and damage to beamline components can result in a high cost. Finally, the cell must be compact enough to reside in a small space, frequently less than 0.5 m in any direction. Ideally, a packed-bed reactor that would require

little modification from an experimental reactor setup could be used as the cell to best approximate the behavior of the catalyst under test reaction conditions in a laboratory.

Typical cells for *in situ* absorption spectrum measurement such as the Nashner-Adler[6] and Clausen[7] cells are now limited by their ability to collect only one sample at a time. While the Nashner-Adler cell allows for the collection of spectra at high temperature and under a flowing gas atmosphere, it also requires that the sample be pressed into a fragile, self-supported wafer. The flowing gas moves around the pellet, preventing the cell from being used for operando studies, and the large Kapton film windows have a limited pressure tolerance. The Clausen cell design can be used for operando studies, but is limited by the sample size that can fit inside the narrow reactor tube, and requires a tradeoff between temperatures that can be reached and X-ray energy that can be transmitted through the the reactor material. The samples in both cells are heated from only one side, which could result in temperature gradients within each sample. A sample cell that more closely resembles a catalytic reactor would offer a significant improvement to *in situ* and operando reaction studies.

Past designs for high throughput collection of X-ray absorption spectra include a sample holder capable of holding up to 6 self-supported wafers in flowing gas,[1] or from an 8-well microreactor that could be used to collect spectra *in situ* with control over the common gas flowed through each well.[8] These cells, like many others in the literature, have unusual reactor configurations or require structural modification of the catalyst powder such as pelletization that would not be compatible with *operando* study. Aside from multiple-sample-holder-setups, multi-channel ionization chambers have been designed.[9] In the example by Ravel et al., a multi-channel detector was used for the simultaneous measurement of Re standards and the temperature programmed reduction of Ni/Al_2O_3 catalysts using H_2, demonstrating the effect of precursor on

the Ni reducibility.[10] This type of design offers the possibility of truly simultaneous *operando* measurements, provided the samples can be packed in a small enough space and exposed to the desired reaction conditions.

To meet the need for both a high-throughput and *in situ* or *operando* capable reactor, a cell was designed to perform a wide variety of measurements on up to four samples in quick succession under a flexible range of temperature, pressure, and flowrate conditions. The cell designed herein draws from several past designs that have been used to investigate heterogeneous catalysts in packed bed reactors, including designs by Bare et al.,[11,12] Fingland et al.,[13] Shou and Davis,[14] and Hoffman et al.[15] It also takes advantage of the long-range fast-motion stage available at beamline 8-ID, housed in Brookhaven National Laboratory's NSLS-II. The functionality of the cell has been demonstrated by performing a temperature-programmed reduction (TPR) of various transition-metal-promoted Mo/SiO_2 catalysts using H_2, and comparing results to those obtained from standard H_2-TPR that measures H_2 consumption.

2. Experimental and Cell Construction

2.1. XAS Measurements

The *in situ* reactor cell was operated at beamline 8-ID of the National Synchrotron Light Source II (NSLS-II) at Brookhaven National Lab. The storage ring operates at 3.0 GeV, and had a beam current of approximately 325 mA. The beamline X-ray source uses a high-power damping wiggler to deliver a high flux of photons. The beamline monochromator is driven by a direct drive servo motor for continuous scanning, allowing for subsecond scans over full spectral range of about 1000 eV. The beamline used an X-ray beam diameter of 0.4 mm. *In situ* H_2-TPR probed by X-ray absorption spectroscopy was carried out at the Mo K-edge at 20 keV. To perform the *in situ* temperature programmed reduction, 60 mg of metal-promoted 4 wt.% Mo (containing M:Mo of

1:4, Pd, Cu, Ag, or Ni) was loaded into each tube in the *in situ* reactor. The catalyst beds were sandwiched between two plugs of graphite wool (AvCarb Felt G200). Using a steel rod, one plug of graphite wool was positioned inside the reactor tube offset from the center of the tube by approximately half of the expected catalyst bed thickness. The catalyst powder was added to the reactor tube by pouring through a small paper funnel in a vertical orientation, and then the second graphite wool plug was positioned against the catalyst bed using a steel rod. The plugs were gently compacted against the catalyst bed from both sides to ensure the bed was fixed in position. The homogeneity of the sample was assessed using horizontal and vertical line scans (see Figure S.4 in the supplementary material) to ensure that regions of the sample with uniform X-ray absorption were investigated. More information about sample preparation can be found in the supplementary material. Before beginning the H_2-TPR, each tube of the reactor cell was flushed with He at 20 cm^3 min^{-1} for 10 min. The gas flow was then switched to 6% H_2/He at 20 cm^3 min^{-1} and the cell temperature was increased linearly from 298 K to 700 K at a rate of 5 K min^{-1}. Scans were taken every 45 s, for a temperature differential between subsequent scans of the same sample of approximately 15 K.

2.2. Catalyst Preparation and Characterization

Supported Mo catalysts promoted by Pd, Cu, Ni, and Ag were prepared by a sequential incipient wetness impregnation method. A loading of 4 wt.% Mo (ammonium heptamolybdate tetrahydrate, Strem Chemicals, 99.98%) was added to 5 g of high-surface-area SiO_2 (Fuji Silysia Chemical Ltd., 0.72 cm^3 g^{-1}, 511 m^2 g^{-1}) by impregnating the support to the point of incipient wetness and mixing until the solution was homogeneously distributed throughout the support particles. The mixture was dried overnight at 383 K, before it was heated to 773 K over 3 h in flowing air at 100 cm^3 min^{-1}, treated in flowing air at 773 K for 3 h, then cooled to room

temperature (298 K). After Mo was added, a promoter (Pd, Cu, Ni, or Ag) was added using the same procedure (using solutions of tetraaminepalladium(II) nitrate, 10 wt%, Aldrich, copper(II) nitrate trihydrate, Sigma Aldrich, 99-104%, nickel(II) nitrate hexahydrate, Aldrich, 99.999%, or silver nitrate, Sigma Aldrich, ≥99.0%, which was added under low-light conditions) in a ratio of 1 promoter atom to every 4 Mo atoms resulting in 1 wt.% Pd or Ag or 0.6 wt.% Cu or Ni promotion. Catalysts were stored under ambient conditions prior to use.

Temperature programmed reduction using 5% H_2 in Ar (Praxair, certified mixture) (H_2-TPR) was carried out using a Micromeritics Autochem II 2920 with thermal conductivity detector (TCD). A U-shaped reaction tube was loaded with 100 mg of the as-synthesized catalyst, which was supported on a bed of quartz wool. The sample temperature was ramped at a rate of 10 K min^{-1} in 50 cm^3 min^{-1} 5% H_2 in Ar over a temperature range from 305 to 1273 K. Effluent gas was flowed through a stainless-steel loop submerged in a dry-ice and 2-propanol cooling bath to trap water before feeding the dried gas to a thermal conductivity detector (TCD). The inverse TCD signal (indicative of H_2 consumption) and temperature were recorded as a function of time.

2.3. Reactor Tube and Window Construction

All parts discussed in this section are summarized in

Table **1**. Dimensions of the cell components are reported herein using imperial units to be consistent with units used to manufacture and purchase the components used for construction. The tubular reactors are designed to be able to retain a bed of catalyst powder in the X-ray beam in the same configuration as a typical lab-scale packed-bed reactor by orienting the catalyst bed horizontally and transmitting the X-ray beam through the length of the bed. The reactor design is shown in Figure 1. Here, each reactor is a 6-in. long, 1/4-in. O.D. 316 stainless steel tube (Swagelok SS-T4-S-035-20). A variety of materials can be used, however, including stainless steel, graphite, or beryllium if desired. The tubular reactors are attached to three-way tees (Swagelok SS-400-3-4TFT) at the inlet and outlet of each tube as shown in Figure 1. A 1/4-inch male NPT (MNPT) to VCR fitting (Swagelok SS-4-VCR-1-4) used to fix the windows to the ends of the reactors. The reactor tubes are swaged to the tees opposite the FNPT fittings, and a 1/4-inch reducing port fitting to 1/8-inch tube adapter (Swagelok SS-401-PC-2) was fixed to the perpendicular at the tee. A Swagelok 1/8-inch quick-connect (Swagelok SS-QM2-B-200 or SS-QM2-D-200) was attached to the 1/8-inch tube adapter to allow for easy connection/disconnection of each reactor individually. At each end of the reactor tube, the three-way tee could be inserted into a bracket that held up to four of the tubes in line with the long direction of the reaction cell base plate. A small screw on the top of each bracket was used to hold the tubes in place during use by compressing the 3-way tees at the end of each tube together. This was necessary to avoid rotating the tubes and moving the sample while the beamline's moving stage was in use. The base of the bracket was mounted to a 1/2-inch thick aluminum baseplate, where it sat in two machined grooves that allowed the brackets to slide to or from the center of the baseplate, to facilitate mounting the four tubes in the center of the heating block. Reactant gases were supplied to each tube independently via an array of four MKS GE 50A mass flow controllers. Flexible copper

tubing leading from the flow controllers to the reactor cell allowed for unimpeded vertical motion of the cell to align each set of windows with the X-ray beam path.

Table 1: Summary of parts used to build the high-throughput XAS cell.

Item name	Supplier	Part number	Description
Miniature quick connect body/stem, 0.05 Cv, 1/8-inch Swagelok tube fitting	Swagelok	SS-QM2-B-200, SS-QM2-D-200	Quick connects for gas inlets/outlets on reactor tubes
1/4-inch to 1/8-inch tube adapter		SS-401-PC-2	Reducing port adapter for reactor quick connects
1/4-inch tube O.D. to 1/4-inch-FNPT (3-way tee)		SS-400-3-4TFT	Connection tee to transmit X-ray beam and gas flow through reactor
1/4-inch O.D. tube		SS-T4-S-035-20	Used in 6-inch segments to produce the reactor tubes
1/4-inch VCR to 1/4-inch MNPT		SS-4-VCR-1-4	X-ray path connection for window apparatus to reactor tube
1/4-inch VCR nut		SS-4-VCR-1	Compression fitting for window
1/2-inch O.D. stainless steel washer, 0.17-inch I.D.	McMaster Carr	91525A318	Mechanical support for window
1/2-inch O.D. Viton washer, 0.17-inch I.D.		93412A407	Viton sealing o-ring for window
Kapton window, 0.001, 0.02 inch thick		2271K1 - 7161T21	X-ray transparent windows
Threaded rods		93250A215	For mounting heating jacket
Aluminum bars		8975K324, 9246K21, 8982K885, 9246K484	For machining heating jacket and cell base.
Calcium silicate insulation, 1/2-inch thick		9353K31	Rigid insulation
Heating cartridges, 3/8-inch O.D.	Thermal Devices, Inc.	E2A55-L12	Insertable heating cartridges

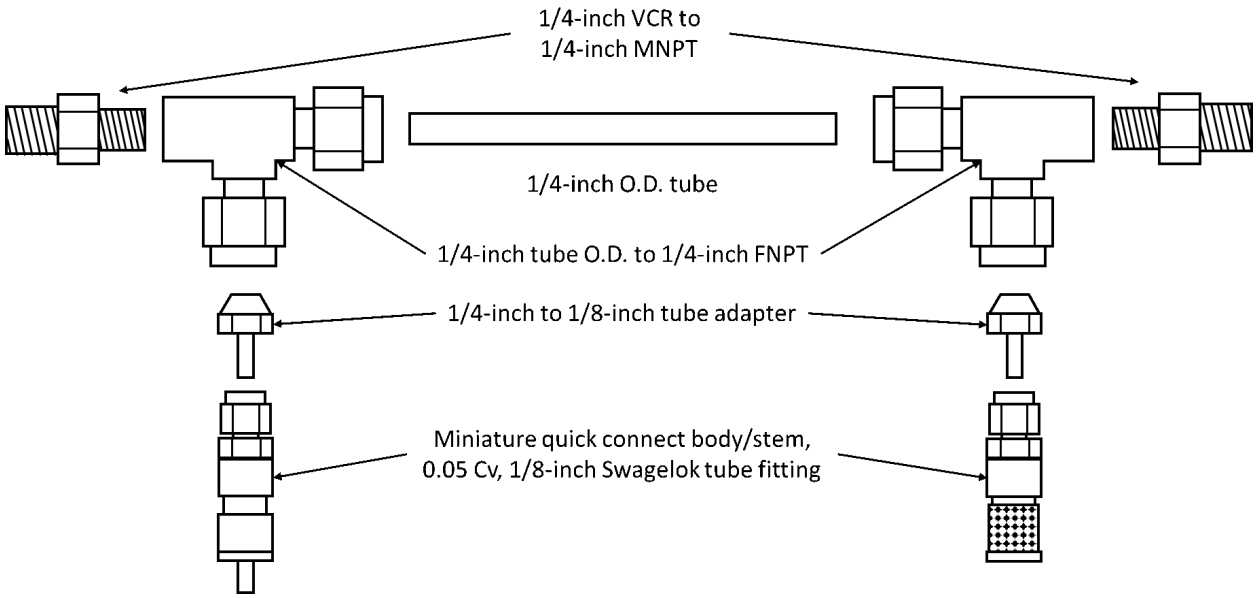

Figure 1: Design of the reactor tube used for the in situ collection of X-ray absorption spectra.

The FNPT fittings at the ends of the two reactor three-way tees were used to mount the cell windows, which were attached to the two 1/4-inch MNPT to 1/4-inch VCR adapters. A 1/2-inch diameter hole punch was used to produce 1/2-inch diameter circular pieces of Kapton. Instead of a VCR seal, a 1/2-inch O.D. Viton washer with I.D. 0.17 inches (the inner diameter of the 1/4-inch reactor tube), the Kapton window, and a stainless-steel washer of the same dimensions as the Viton washer were placed inside the VCR nut in the configuration shown in Figure 2. When the VCR nut was tightened onto the VCR fitting, the stainless-steel washer and Kapton window were compressed against the Viton washer from the outside of the cell, while the VCR fitting sealing surface pressed against the Viton washer from the inside of the cell, creating a gas-tight seal that was capable of withstanding pressures of over 2 MPa when 0.02-inch Kapton windows were used. This modular window design was chosen to provide flexibility with regard to the reactor pressure,

as changing reactor windows can be done rapidly and all windows and sealing materials used can be re-used. The window design is shown in Figure 2.

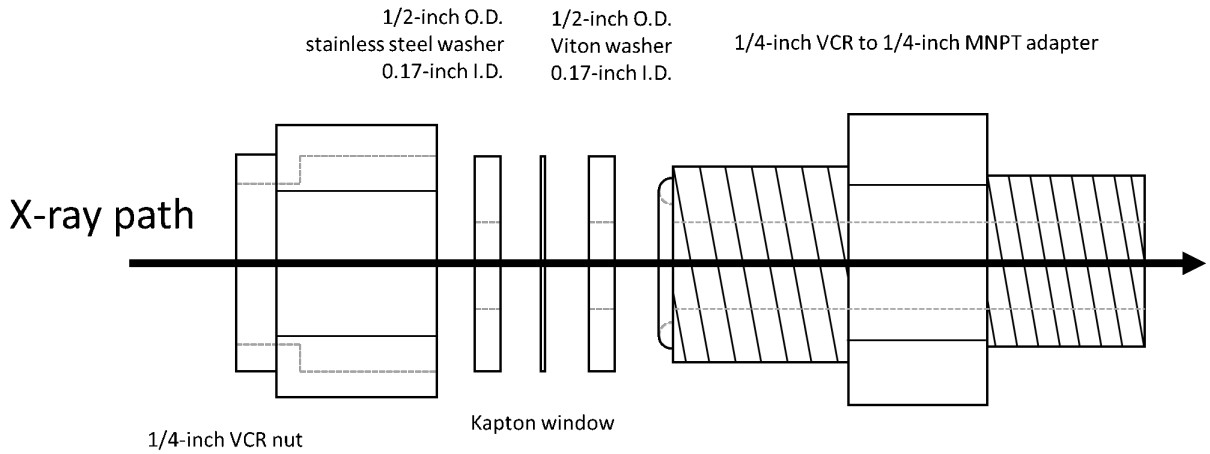

Figure 2: Design of the modular windows for the reactor tubes used for the in situ collection of X-ray absorption spectra.

2.4. Heating Block Design

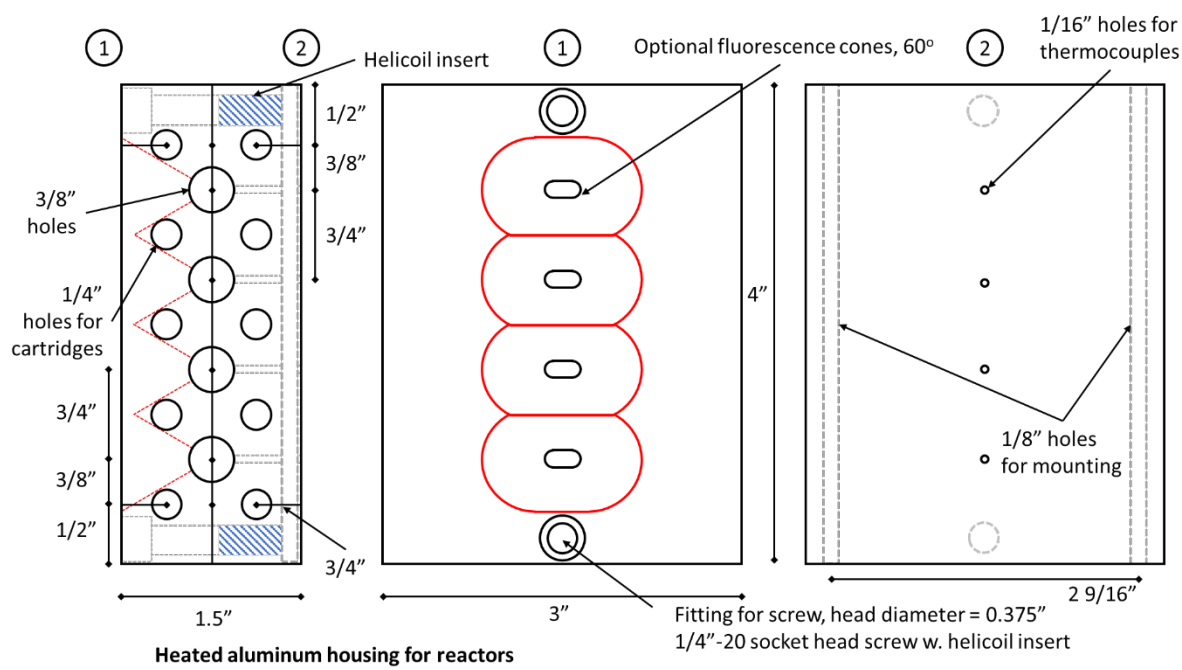

Figure 3: Design of the aluminum reactor cell heating block, shown with optional drilled fluorescence cones.

An aluminum block 3 inches by 4 inches by 1.5 inches was machined to the specifications in Figure 3 for use as a heating jacket for the reactor tubes. Four 3/8-inch diameter holes were drilled through the block along the centerline of the 1.5-inch-wide face of the block to allow the reactor tubes to sit inside the aluminum block as shown in Figure 4 (top and middle). The block was then cut in half vertically, splitting the reactor through-holes into two halves, designated (1) and (2) in Figure 3. A total of 10 holes were drilled on the 1.5-inch wide side, 2.5 inches deep, to allow for the 10 1/4 inch OD cartridge heaters to be inserted into the aluminum block. On the 3-inch by 4-inch faces, 4 holes were drilled through to allow for a 1/16-inch thermocouple to be inserted into the center of each of the reactor channels to measure the temperature on the external surface of each reactor tube. At the top and bottom of this face, a fitting was made for a 1/4-20 bolt to hold the two halves of the heating block together. Steel helicoil inserts in these two fittings were added to prevent the malleable aluminum fittings from being stripped during repeated use. Vertical 1/8-inch holes were drilled through the block to hold the heating block in place around the reactor tubes as shown in Figure 3 and Figure 4 (complete assembled cell). The heating block was also insulated with 0.5-inch-thick calcium silicate insulation, machined to fit flush around the through-block fittings. The heating block sat on a piece of calcium silicate insulation that was supported by 4 stainless steel legs attached to the baseplate. On side (2) (see Figure 3), two 1/8 inch threaded rods were inserted through the entire heating block, insulation layer, and mounting legs through the 1/8-inch mounting holes, which held the heating block in place vertically.

The 10 cartridge heaters were inserted into the aluminum block in the 10 cartridge holes discussed earlier. The electrical leads for each cartridge were attached in parallel to a terminal block mounted on the cell baseplate and covered by a rubber flap to prevent accidental contact with the terminal block during operation of the cell. Power was supplied through a connection

from the terminal block to a grounded NEMA 5-15P connector. The ground wire of the NEMA 5-15P connector was attached to the cell baseplate. The temperature was controlled using an Omega CN7800-series PID controller equipped with a solid-state relay to supply heating power from a 120 V source.

Optionally, conical slits could be drilled into the heating block on one side as shown in Figure 3, allowing for the use of an X-ray transparent tube (e.g. graphite, beryllium) to collect fluorescence spectra from the catalyst bed. The vertical vertex angle of each cone was 60 degrees measured from the center of the reactor channel in the heating block, to avoid intersecting the channels containing the heating cartridges.

Performance of the heating block was validated by varying the temperature measured at the outside of the reactor tube using the drilled channel in the heating block. The temperature inside the reactor tubes was measured with 25 cm^3 min^{-1} of He flowing through each tube by removing the Kapton window from the downstream end of each reactor tube and inserting a 1/16 inch thermocouple into the cell. A 1/16-inch ferrule swaged to the thermocouple to prevent the thermocouple tip from contacting the reactor walls. The results of the validation are shown in Figure 5(a), with He flowing from high thermocouple distances to low thermocouple distances (right to left, as shown). Thermocouple distances from 11 cm to 19 cm fall within the insulated block, with a thermocouple distance of 15 cm corresponding to the center of the block. The central point reached the highest temperature, with some asymmetry on either side likely due to heat transport by convection through the flowing gas. This hottest point was from 8-23 K below the setpoint temperature depending on the setpoint. A correction based on measured temperature can be found in Figure 5(b). The points at 12.5 and 17.5 cm fell within the insulation on either end of the block, indicating only slight temperature decrease within the heating block. Outside the

insulated section of the block at 10 cm and 20 cm, the temperature begins to drop rapidly. Once the windows are reached, the reactor tube temperature remains only 5-10 K higher than the external temperature. The heating block that was tested was constructed out of aluminum, which should not be heated above 773 K during the cell operation as the melting point of aluminum is 933 K. However, replacement of the block with one made from a more temperature-resistant material or ceramic furnace would increase the maximum allowed temperature of the cell.

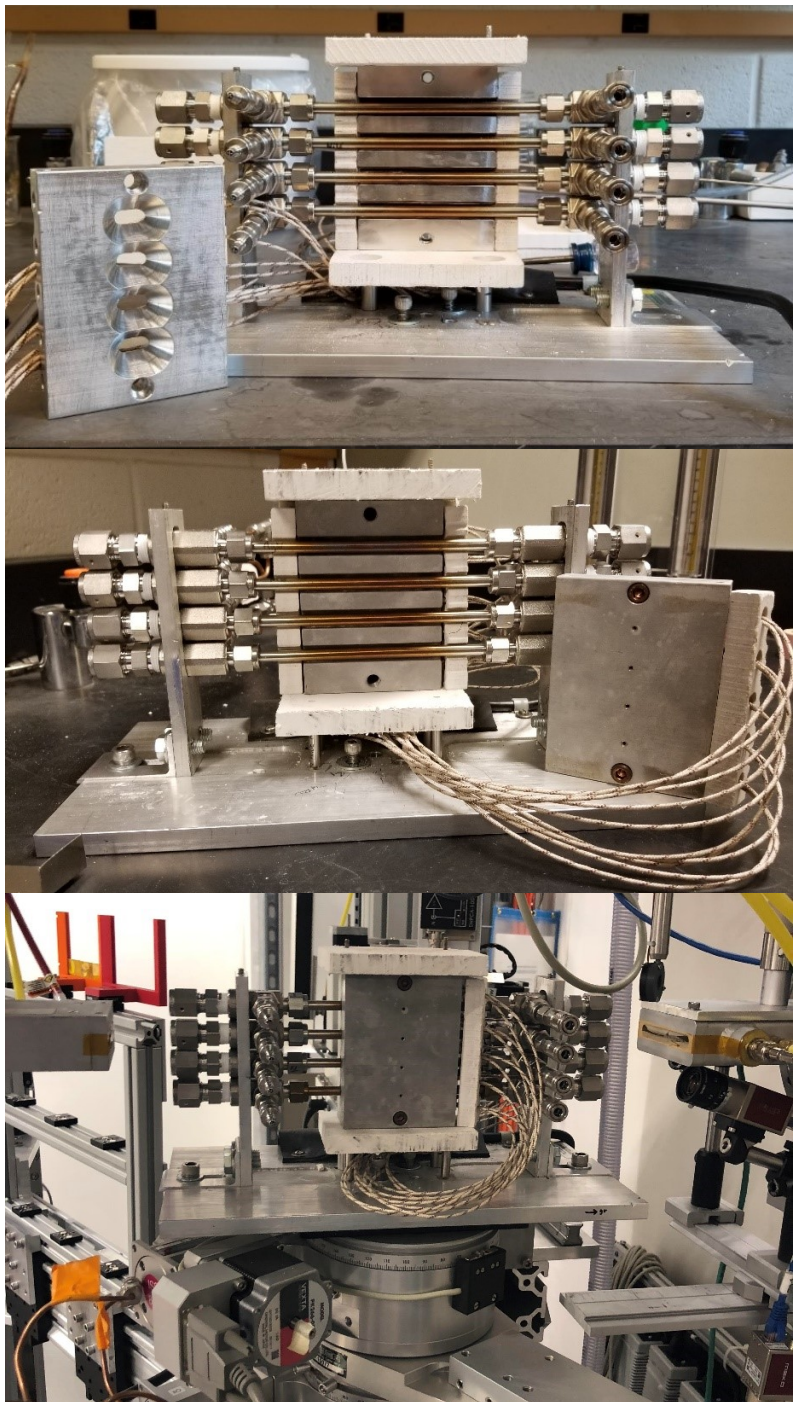

Figure 4: **Top, Middle:** ***Completed reactor cell, with (top) and without (middle) optional fluorescence cones drilled in the heating block.*** **Bottom:** ***Reactor cell sitting on the goniometer (rotating stage) in the hutch at 8-ID, after alignment of the tubes with the X-ray beam. Some of the insulation has been removed to display the aluminum transmission heating block with 1/16-inch holes for thermocouple insertion.***

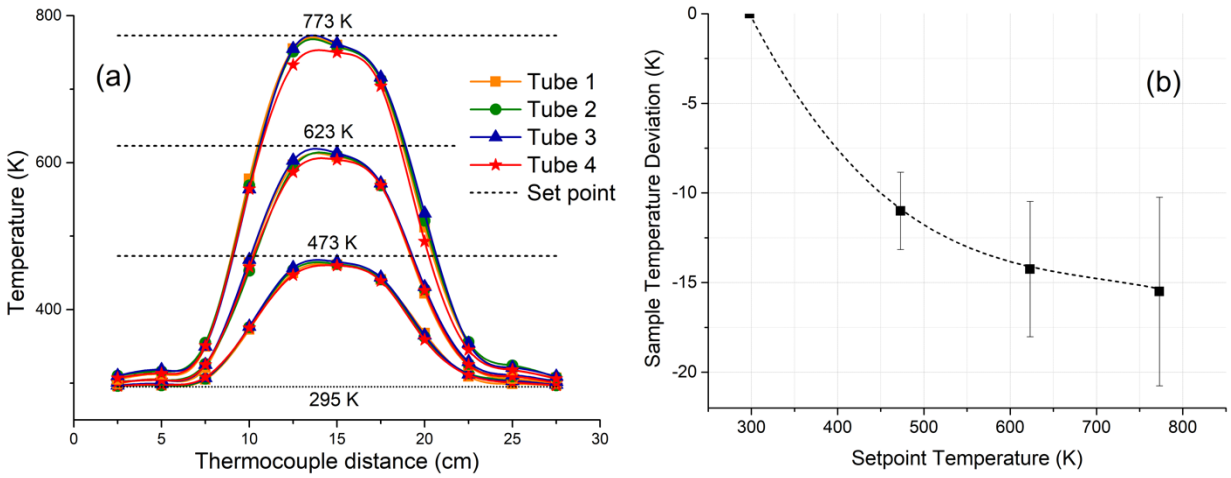

Figure 5: (a) Validation of the performance of the heating block for the in situ cell, showing the temperature measured in the center of each reactor tube at positions along the length of the reactor as the setpoint was varied and He was flowed through each tube from right to left (high to low thermocouple distance). (b) Deviation of the hot zone temperature from the set point temperature, with dashed line to indicate the trend.

3. Results and Discussion

3.1. Temperature-Programmed Reduction

Temperature programmed reduction using a TCD to detect H_2 was carried out to determine if various reducible metal promoters resulted in differing oxidation states of Mo. The H_2-TPR results are summarized in Figure 6, where it is evident that H_2 consumption alone is not enough information to directly determine the Mo oxidation state. The H_2-TPR study revealed that there are a number of H_2 consumption peaks in each of the M-promoted Mo catalysts, each of which might correspond to the reduction of at least one metal component of each catalyst. The Pd-promoted Mo began to reduce in H_2 at near-ambient conditions, as low as 320 K. This behavior is expected for Pd-containing materials, indicating reduction of PdO in the as-synthesized material. Subsequent H_2 consumption peaks appeared at 490 K, and then as a broad feature from 700 to

1100 K containing at least two distinct reduction features. The Cu-promoted Mo demonstrated reached a maximum H_2 consumption at 520 K indicative of reduction of CuO,[16] followed by continued H_2 consumption over the range of the temperature treatment. The Ag-promoted Mo demonstrated a lower-temperature pair of H_2 consumption peaks around 390 K and 410 K, consistent with reduction of Ag_2O to Ag,[17] followed again by continuous H_2 consumption over the range of the temperature treatment. The Ni-promoted Mo demonstrated no H_2 consumption until 640 K consistent with reduction of NiO,[18] reaching a maximum at 690 K, followed again by sustained H_2 consumption over the range of the experiment in at least two distinct consumption peaks. In each case, it appeared that the promoting metal must be reduced in order to promote any reduction of the Mo component.

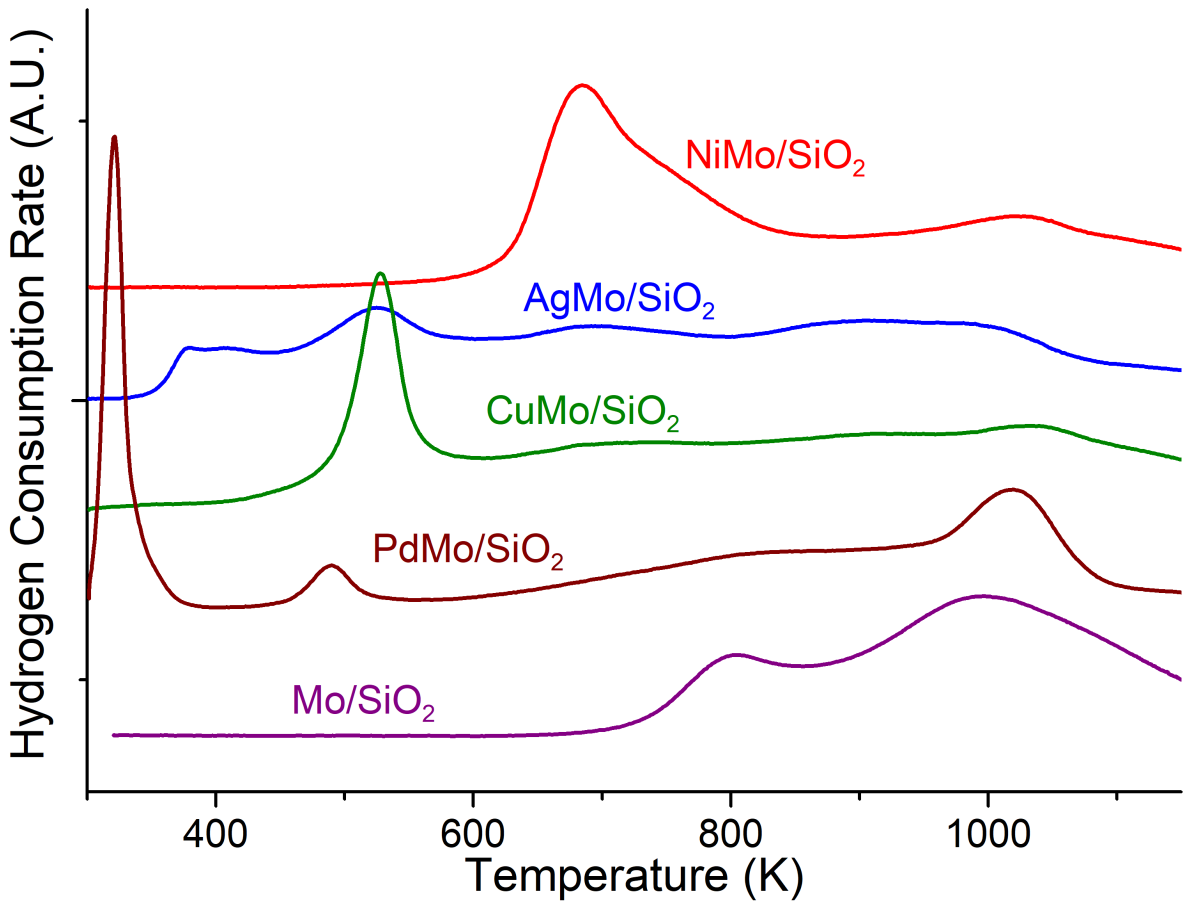

Figure 6: Temperature programmed reduction of M-promoted MoO_x/SiO_2 catalysts. Reduction profiles have been offset for clarity.

3.2. *In Situ* X-Ray Absorption Spectroscopy

In situ X-ray absorption spectroscopy was used to determine the oxidation state of the Mo in the Pd, Cu, Ag, and Ni-promoted Mo/SiO_2 materials as a function of H_2 treatment temperature (Figure 7). The oxidation state of metal-promoted Mo/SiO_2 during H_2-TPR *in situ* in the high-throughput XAS cell was determined by the position of the Mo K-edge absorption edge energy at a normalized height of 0.5. Based on these results, it is evident that Pd-promoted Mo undergoes low-temperature reduction upon exposure to H_2, followed by a small reduction feature at about 480 K and then sustained reduction above 550 K. Both Cu- and Ag-promoted Mo begin to reduce

at above 500 K, with very similar reduction behavior. As suggested by H_2-TPR earlier, Ni-promoted Mo does not undergo reduction until after NiO is expected to be reduced at above 640 K.

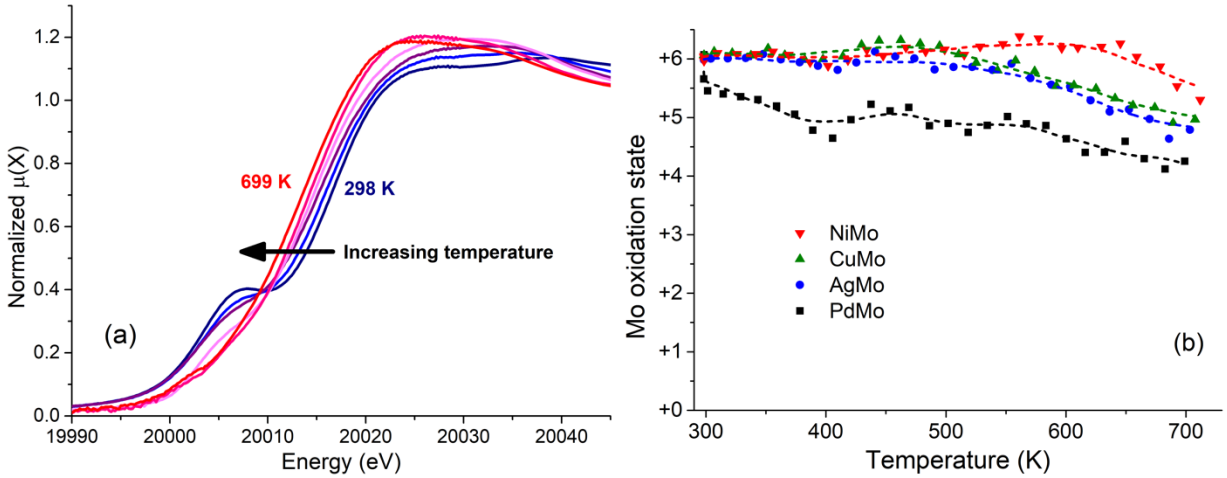

Figure 7: (a) Mo K-edge XANES of PdMo/SiO₂ measured during H₂-TPR using 6% H in He to demonstrate observed change in the Mo K-edge position. (b) Experimentally determined oxidation state of 4% Mo/SiO₂ promoted by Ni, Cu, Ag, and Pd during near-simultaneous temperature programmed reduction in 6% H₂ in He from 298 K to 710 K. Dashed lines are to indicate trends.

The X-ray absorption fine structure spectra that were collected during *in situ* H_2-TPR could also be qualitatively analyzed. A total of 120 EXAFS spectra were obtained for all 4 samples during the 2-hour H_2 TPR. Qualitative information was obtained from the intensities and peak positions from the Fourier transform of the k-space EXAFS oscillations over a k-range of 2.3 to 12 $Å^{-1}$.[19] A subset of the EXAFS spectra and corresponding Fourier transforms collected during *in situ* H_2-TPR of $PdMo/SiO_2$ is shown in Figure 8. Results from the XANES indicated that reduction of Mo began immediately after beginning the H_2 feed. Correspondingly, the shortest Mo-O scattering path intensity immediately decreased upon exposure to H_2. Initially, Mo-O and Mo-Mo

scattering paths (at 1.2 Å and 3.2 Å, respectively, without phase-shift correction) were present. Upon exposure to H_2, the shorter Mo-O scattering path transformed into at least 2 overlapping Mo-O scattering paths at slightly longer distances and a Mo-Mo scattering path at 3.7 Å. This structure remained fairly constant intensity from 343 K to 486 K. Above 486 K, the Mo-Mo scattering path intensity began to decrease, and disappeared at 534 K. This is attributed to the spreading of MoO_x clusters across the surface of SiO_2, which has been observed previously.[20,21] Above 534 K, the Mo-O scattering paths continue to decrease in intensity, and the longer Mo-O multiple scattering path almost completely vanished by 683 K. The two temperature regimes where H_2 consumption occurs according to H_2-TPR results collected using thermal conductivity measurements agrees well with the oxidation states observed in the XANES as well as the qualitative analysis of the EXAFS.

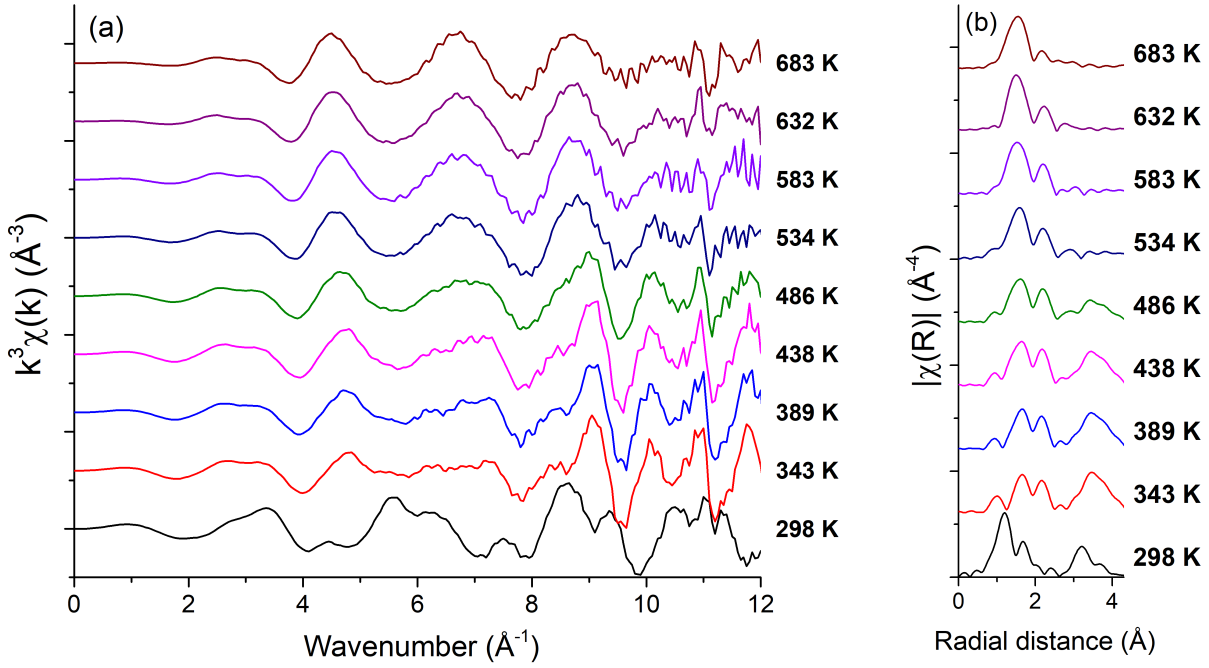

Figure 8: Extended X-ray absorption fine structure spectra (a) in k-space and (b) the corresponding magnitude of the Fourier transform (not phase-shift corrected) of PdMo/SiO_2 during H_2-TPR.

3.3. Reactor Cell Design: Advantages and Disadvantages

The *in situ* reactor cell designed consists of four 1/4 inch outer-diameter reactor tubes, supported horizontally in an aluminum heating block which was modeled off of designs created by Fingland et al.[13] who designed a cell for simultaneous measurement of X-ray absorption spectra and *operando* reaction kinetics. Our cell was prepared for *operando* use by allowing the catalyst bed to consist of free catalyst powder (particle sizes less than 180 μm preferred), packed between two beds of X-ray transparent material such as small amounts of glass or graphite wool, and transmitting the X-ray beam along the axis of the reactor tube (which includes transmission through the reacting gas). To minimize distortion of the absorption spectra, catalyst particle sizes should be kept as small as possible without creating a significant pressure drop across the catalyst bed. Further considerations for sample preparation can be found in the supplementary material. While we have not yet performed any *operando* measurements of catalytic activity using this cell, the design was created with *operando* measurements in mind. Gas mixtures can be supplied independently to each tube, and the effluent of each reactor tube can be collected individually. Therefore, this cell may be used at a beamline with infrastructure available for product analysis. Configuration of the reactor cell in this orientation comes with several advantages and disadvantages. One advantage of this design is that brittle or toxic reactor tube materials like graphite, thin quartz, or beryllium are not required to obtain transmission spectra. Using stainless steel tubing for the reactors allows for the potential use of this system under conditions that mimic reaction conditions exactly, including elevated pressures and temperatures. Another advantage of the design is its mechanical simplicity. The stainless-steel reactor tubes can be substituted for any material that is appropriate for the desired study, and the windows can be easily exchanged with other X-ray transparent materials to meet the need for various pressure ranges or chemical

compatibility with reactants. Reactor tubes can be easily added or removed using the quick-connect fittings. As the reactor tubes are only heated in the reaction zone, the window composition is not strictly limited to materials that are resistant to extreme temperatures.

On the other hand, transmission of the X-ray beam through a long, narrow tube limits the accuracy of temperature measurement by preventing measurements using a thermocouple inserted from one end of the reactor tube into the catalyst bed. Instead, temperature must be measured externally using a thermocouple in contact with the outside of the reactor tube. Additionally, the tube must be aligned precisely to allow transmission along the path of the reactor tube and window fittings. Using the movable sample stage at beamline 8-ID at NSLS-II, this alignment can be performed within minutes, but it may present a challenge to align without precise motion control. Additionally, consideration must be given to the reactant gas mixture. Heavy inert gases such as Ar have a considerable absorption at ambient pressure and at the transmission length of the reactor when using softer X-ray energies. Care should also be taken during packing of the catalyst bed in the reactor cell. If the catalyst bed is not well-packed, or higher flowrates of gas are used, settling of the reactor bed can occur, allowing channeling of the reactants through the top of the reactor bed. Poor packing may also cause the catalyst bed to move out of the heated zone. While the cost of this cell was approximately $3000 in parts, machine labor and beamline infrastructure to accommodate the cell (including mass flow controllers, temperature controllers, etc.) must also be considered as construction costs. A programmable movable stage is also required to utilize the cell to its full capacity.

4. Conclusions

An *operando*-ready reactor cell was designed and constructed to allow XAS measurements using packed beds of sample powders. The reactor cell consists of four parallel tubes with windows

at both ends of the tube, allowing for X-ray beam transmission through the catalyst bed. Each of the four tubes in the reactor cell is supplied by its own gas inlet, allowing for the simultaneous performance of up to four independent experiments. Transmission windows can be easily adjusted for chemical compatibility or to perform experiments using reaction pressures of up to 2 MPa. The cell provides a flexible platform for sample analysis, but it remains incumbent upon the user to adequately prepare their unique sample for analysis. An aluminum heating block allows for reaction temperatures of up to 773 K, but this temperature is only limited by the material of the heating block itself. Performance of the cell in transmission mode was verified by a simple H_2-TPR of Pd, Cu, Ag, and Ni-promoted Mo/SiO_2 catalysts, allowing the oxidation state of the Mo component of each catalyst to be determined as a function of temperature during the TPR using both XANES and qualitative EXAFS analysis.

Supplementary Material

A discussion of catalyst powder sample preparation is included in the supplementary material.

Acknowledgements

Dr. Klaus Attenkofer is acknowledged for his assistance with beamline operations during cell testing. Ricky Buchanan (UVA Engineering) is acknowledged for his role in the machining and design consultation for the heating block and mounting brackets for the reactor tubes. Helpful conversations with Nicholas Kaylor and Jiahan Xie are also acknowledged. This work received funding from MAXNET Energy and the University of Virginia, and used beamline 8-ID of the National Synchrotron Light Source II, a U.S. Department of Energy (DOE) Office of Science User Facility operated for the DOE Office of Science by Brookhaven National Laboratory under Contract No. DE-SC0012704.

References

(1) Jacobs, G.; Ji, Y.; Davis, B. H.; Cronauer, D.; Kropf, A. J.; Marshall, C. L. Fischer-Tropsch Synthesis: Temperature Programmed EXAFS/XANES Investigation of the Influence of Support Type, Cobalt Loading, and Noble Metal Promoter Addition to the Reduction Behavior of Cobalt Oxide Particles. *Appl. Catal. A Gen.* **2007**, *333* (2), 177–191, DOI 10.1016/j.apcata.2007.07.027.

(2) Tsakoumis, N. E.; Voronov, A.; Ronning, M.; Beek, W. Van; Borg, O.; Rytter, E.; Holmen, A. Fischer-Tropsch Synthesis: An XAS/XRPD Combined in Situ Study from Catalyst Activation to Deactivation. *J. Catal.* **2012**, *291*, 138–148, DOI 10.1016/j.jcat.2012.04.018.

(3) Alayon, E. M. C.; Nachtegaal, M.; Kleymenov, E.; Van Bokhoven, J. A. Determination of the Electronic and Geometric Structure of Cu Sites during Methane Conversion over Cu-MOR with X-Ray Absorption Spectroscopy. *Microporous Mesoporous Mater.* **2013**, *166*, 131–136, DOI 10.1016/j.micromeso.2012.04.054.

(4) Bordiga, S.; Groppo, E.; Agostini, G.; van Bokhoven, J. A.; Lamberti, C. Reactivity of Surface Species in Heterogeneous Catalysts Probed by In Situ X-Ray Absorption Techniques. *Chem. Rev.* **2013**, *113* (3), 1736–1850, DOI 10.1021/cr2000898.

(5) Palomino, R. M.; Stavitski, E.; Waluyo, I.; Chen-Wiegart, Y. chen K.; Abeykoon, M.; Sadowski, J. T.; Rodriguez, J. A.; Frenkel, A. I.; Senanayake, S. D. New In-Situ and Operando Facilities for Catalysis Science at NSLS-II: The Deployment of Real-Time, Chemical, and Structure-Sensitive X-Ray Probes. *Synchrotron Radiat. News* **2017**, *30* (2), 30–37, DOI 10.1080/08940886.2017.1289805.

(6) Nashner, M. S.; Frenkel, A. I.; Adler, D. L.; Shapley, J. R.; Nuzzo, R. G. Structural Characterization of Carbon-Supported Platinum-Ruthenium Nanoparticles from the

Molecular Cluster Precursor PtRu 5 C(CO) 16. *J. Am. Chem. Soc.* **1997**, *119* (33), 7760–7771, DOI 10.1021/ja971039f.

(7) Clausen, B. S.; Steffensen, G.; Fabius, B.; Villadsen, J.; Feidenhans'l, R.; Topsøe, H. In Situ Cell for Combined XRD and On-Line Catalysis Tests: Studies of Cu-Based Water Gas Shift and Methanol Catalysts. *J. Catal.* **1991**, *132* (2), 524–535, DOI 10.1016/0021-9517(91)90168-4.

(8) Tsapatsaris, N.; Beesley, A. M.; Weiher, N.; Tatton, H.; Dent, A. J.; Mosselmans, F. J. W.; Tromp, M.; Russu, S.; Evans, J.; Harvey, I.; et al. High Throughput in Situ XAFS Screening of Catalysts. *AIP Conf. Proc.* **2007**, *882*, 597–599, DOI 10.1063/1.2644604.

(9) Ravel, B.; Scorzato, C.; Siddons, D. P.; Kelly, S. D.; Bare, S. R. Simultaneous XAFS Measurements of Multiple Samples. *J. Synchrotron Radiat.* **2010**, *17* (3), 380–385, DOI 10.1107/S0909049510006230.

(10) Bare, S. R.; Kelly, S. D.; Ravel, B.; Greenlay, N.; King, L.; Mickelson, G. E. Characterizing Industrial Catalysts Using in Situ XAFS under Identical Conditions. *Phys. Chem. Chem. Phys.* **2010**, *12* (27), 7702, DOI 10.1039/b926621f.

(11) Bare, S. R.; Mickelson, G. E.; Modica, F. S.; Ringwelski, A. Z.; Yang, N. Simple Flow through Reaction Cells for in Situ Transmission and Fluorescence X-Ray-Absorption Spectroscopy of Heterogeneous Catalysts. *Rev. Sci. Instrum.* **2006**, *77* (2), DOI 10.1063/1.2168685.

(12) Bare, S. R.; Yang, N.; Kelly, S. D.; Mickelson, G. E.; Modica, F. S. Design and Operation of a High Pressure Reaction Cell for in Situ X-Ray Absorption Spectroscopy. *Catal. Today* **2007**, *126* (1–2), 18–26, DOI 10.1016/j.cattod.2006.10.007.

(13) Fingland, B. R.; Ribeiro, F. H.; Miller, J. T. Simultaneous Measurement of X-Ray

Absorption Spectra and Kinetics: A Fixed-Bed, Plug-Flow Operando Reactor. *Catal. Letters* **2009**, *131* (1–2), 1–6, DOI 10.1007/s10562-009-0026-8.

(14) Shou, H.; Davis, R. J. Reactivity and in Situ X-Ray Absorption Spectroscopy of Rb-Promoted Mo 2C/MgO Catalysts for Higher Alcohol Synthesis. *J. Catal.* **2011**, *282* (1), 83–93, DOI 10.1016/j.jcat.2011.05.028.

(15) Hoffman, A. S.; Debefve, L. M.; Bendjeriou-Sedjerari, A.; Ouldchikh, S.; Bare, S. R.; Basset, J. M.; Gates, B. C. Transmission and Fluorescence X-Ray Absorption Spectroscopy Cell/Flow Reactor for Powder Samples under Vacuum or in Reactive Atmospheres. *Rev. Sci. Instrum.* **2016**, *87* (7), DOI 10.1063/1.4958824.

(16) Shimokawabe, M.; Takezawa, N.; Kobayashi, H. Characterization of Copper-Silica Catalysts Prepared by Ion Exchange. *Appl. Catal.* **1982**, *2* (6), 379–387, DOI 10.1016/0166-9834(82)80156-5.

(17) Qu, Z.; Huang, W.; Cheng, M.; Bao, X. Restructuring and Redispersion of Silver on SiO2under Oxidizing/Reducing Atmospheres and Its Activity toward CO Oxidation. *J. Phys. Chem. B* **2005**, *109* (33), 15842–15848, DOI 10.1021/jp050152m.

(18) Zhang, L.; Lin, J.; Chen, Y. Studies of Surface NiO Species in NiO/SiO2 Catalysts Using Temperature-Programmed Reduction and X-Ray Diffraction. *J. Chem. Soc. Faraday Trans.* **1992**, *88* (14), 2075–2078, DOI 10.1039/FT9928802075.

(19) Kakuta, N.; Tohji, K.; Udagawa, Y. Molybdenum Oxide Structure on Silica-Supported Catalysts Studied by Raman Spectroscopy and EXAFS. *J. Phys. Chem.* **1988**, *92* (9), 2583–2587, DOI 10.1021/j100320a037.

(20) de Boer, M.; van Dillen, A. J.; Koningsberger, D. C.; Geus, J. W.; Vuurman, M. A.; Wachs, I. E. Remarkable Spreading Behavior of Molybdena on Silica Catalysts. An in Situ EXAFS-

Raman Study. *Catal. Letters* **1991**, *11* (2), 227–239, DOI 10.1007/BF00764089.

(21) Braun, S.; Appel, L. G.; Camorim, V. L.; Schmal, M. Thermal Spreading of MoO3 onto Silica Supports. *J. Phys. Chem. B* **2000**, *104* (28), 6584–6590, DOI 10.1021/jp000287m.